Journal of Chromatography A, 1218 (2011) 6402–6411

Contents lists available at ScienceDirect

Journal of Chromatography A

journal homepage: www.elsevier.com/locate/chroma

Recombinant protein purification using gradient assisted simulated moving bed hydrophobic interaction chromatography. Part II: Process design and experimental validation

Ludmila Gueorguieva[a], Sivakumar Palani[b,c], Ursula Rinas[d,e], Guhan Jayaraman[b], Andreas Seidel-Morgenstern[a,c,*]

[a] Otto-von-Guericke-Universität, Institut für Verfahrenstechnik, P.O. Box 4120, D-39106 Magdeburg, Germany
[b] Indian Institute of Technology – Madras, Department of Biotechnology, Chennai 600036, India
[c] Max Planck Institute for Dynamics of Complex Technical Systems, Sandtorstrasse 1, D-39120 Magdeburg, Germany
[d] Helmholtz Centre for Infection Research, Inhoffenstrasse 7, D-38124 Braunschweig, Germany
[e] Institute of Technical Chemistry – Life Science, Leibniz University of Hannover, Callinstr. 5, D-30167 Hannover, Germany

ARTICLE INFO

Article history:
Received 4 December 2010
Received in revised form 29 May 2011
Accepted 3 July 2011
Available online 18 July 2011

Keywords:
Streptokinase
Hydrophobic interaction chromatography
Two-step gradient open-loop simulated moving bed chromatography

ABSTRACT

In the first part of this work adsorption isotherm parameters were acquired to describe the migration of recombinant streptokinase in Butyl Sepharose columns at different salt concentrations. Based on these results, a simulated moving bed (SMB) chromatographic process was designed and realised, which exploits a two-step salt gradient and allows the continuous separation of streptokinase from contaminants present in a clarified *Escherichia coli* cell lysate solution. This second part describes the design of the three-zone open-loop gradient SMB process applying both equilibrium theory and an equilibrium stage model and presents results of a series of experiments aiming to obtain pure streptokinase. Moreover, the potential of the SMB process and the design approach are evaluated.

1. Introduction

The introduction of an increasing number of protein-based drugs in the market significantly accelerates the development of efficient production methods [1]. With bacterial systems, the target recombinant proteins typically represent about 25% of the total protein in the starting material [2]. In case of insoluble inclusion bodies this percentage reaches 30–70% [3]. Due to the tremendous progress achieved in genetics and molecular biology, the bottleneck in biotechnology is not anymore the overexpression of proteins but their efficient recovery and characterization [4]. In order to meet purity demands set by FDA regulations, the required downstream processing of recombinant proteins needs reliable and high-throughput separation processes. High selectivities can be provided in particular by chromatographic methods, provided suitable stationary phases are available and optimized process concepts are applied. An attractive alternative to overcome the classical restriction of relative low productivity, inherent to conventional batch chromatography, is to use continuous operation concepts applying multi-column counter-current chromatography. Nowadays the classical four-zone simulated moving bed (SMB) process is an established technique and widely used in industry to separate e.g. enantiomers [5–8]. Main advantages of the SMB technique are reduced solvent consumption, increased productivity and higher product concentration, clearly all indicators of reduced production costs [5]. During the last years the SMB technology was applied increasingly for the separation of valuable compounds such as proteins, antibodies and viruses from complex mixtures [9–19]. However, a successful application to the downstream processing of biotechnological products is still challenging due to the complexity of the multi-component feed mixtures and the limitation to only two outlet fractions provided by conventional SMB chromatography. The latter property requires that the target component is either the fastest or the slowest eluting component in the feed. For this reason the process is preferably considered as a capture or polishing step. To tackle the wide retention time spectrum typically encountered in separations of bio-molecules, the application of gradients is a powerful concept [10–12,17]. Modulations of the solvent strength can be made by using different pH-values or salt concentrations in the two inlet streams (feed and desorbent) [e.g. 10–12]. To design such sophisticated gradient processes, knowledge regarding the

* Corresponding author at: Otto-von-Guericke-Universität, Institut für Verfahrenstechnik, P.O. Box 4120, D-39106 Magdeburg, Germany. Tel.: +49 391 6110 4001; fax: +49 391 6110 403.
E-mail address: seidel-morgenstern@mpi-magdeburg.mpg.de (A. Seidel-Morgenstern).

0021-9673/$ – see front matter © 2011 Elsevier B.V. All rights reserved.
doi:10.1016/j.chroma.2011.07.008

distribution equilibria at different elution conditions is essential [10,11,20–22].

In the first part of this communication we discussed the determination of essential adsorption equilibrium constants on a hydrophobic interaction chromatography (HIC) matrix for recombinant streptokinase, the target product present in a E.coli cell lysate [23]. After this preliminary study two linear functions for the equilibrium (Henry) constants as a function of the salt concentration are available for streptokinase (*sk*) and for a lumped impurities fraction (*im*) containing degraded streptokinase (deg *sk*) and cellular contaminants.

The intention of the second part of this communication is the development of a continuous HIC-based gradient SMB process for the purification of recombinant streptokinase. For the design the available adsorption isotherm parameters are the key information. To separate the complex feed mixture applying a two-step salt gradient process, we performed a theoretical study using the equilibrium theory [24–27] and an equilibrium stage model (Craig model) [e.g. 29]. Based on the results, suitable operating conditions were selected for the separation problem considered. Finally a series of experiments was carried out to separate continuously recombinant streptokinase from cell lysate.

2. Three-zone two-step gradient TMB process

The principle of classical simulated moving bed chromatography is characterized by a four-zone arrangement and a closed solvent loop [30]. For the realisation of the process, there are two inlet streams (feed, desorbent) and two outlet streams (extract, raffinate). The four zones in the unit can be identified by their tasks. Zones *II* and *III* separate the feed, continuously introduced in between, into two streams. Zones *I* and *IV* are zones for the regeneration of the solid and liquid phases, needed to allow their direct recycling. This elegant closed-loop four-zone configuration reduces the desorbent consumption, but increases the risk of cross-contamination in case of failure of the regeneration zones. For biotechnological separations often cheap aqueous buffers are used as mobile phase and a simpler three-zone-configuration can be applied [10–15]. To explain the principle a scheme of the corresponding so-called true moving bed (TMB) process is represented in Fig. 1a. In this configuration the three zones have to fulfil the same tasks as the zones *I–III* in the conventional four-zone process. The fourth zone for regeneration of the mobile phase is not required anymore. Furthermore, in the process investigated in this study, a two-step salt gradient is applied (see Fig. 1b). This salt gradient is developed between zones *I*/*II* and zone *III*. In zones *I* and *II* the salt concentration is the same as in the introduced desorbent stream. The gradient in zone *III* is formed by mixing of the feed stream and the internal stream leaving zone *II*.

The study presented here is devoted to the continuous separation of recombinant streptokinase from cell lysate using hydrophobic interaction chromatography (HIC). For the realisation of the required two-step gradient using HIC mode, the salt concentration in the feed stream has to be set higher than in the desorbent stream.

In the configuration shown in Fig. 1 and implemented experimentally two extra zones for additional regeneration and equilibration of the solid phase are applied [13]. These two zones are operated independently and use different mobile phases. In the regeneration zone the stationary phase coming from zone *I* is regenerated with a buffer solution (buffer 1) providing fast elution. The role of this zone is to remove possible contaminants strongly bound on the stationary phase. As suggested in [11] in the equilibration zone the stationary phase is equilibrated with the mobile phase

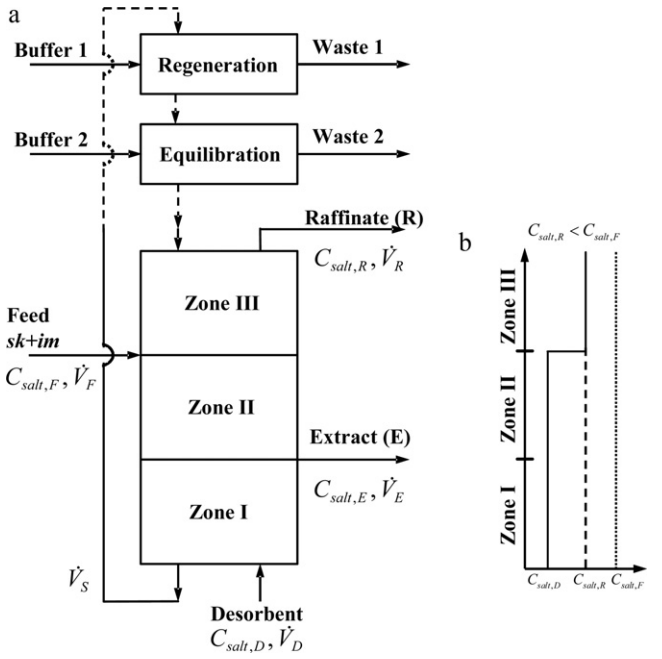

Fig. 1. (a) Scheme of a three-zone open-loop gradient TMB process with implemented regeneration and equilibration zones; (b) corresponding two-step salt gradient as applied using HIC chromatography.

composition leaving as raffinate zone *III* (buffer 2). This equilibration is useful to avoid the formation of unwanted mobile phase gradients within zone *III*.

The three-zone open-loop configuration represented in Fig. 1 was shown to be applicable and attractive for the separation of proteins from mixtures containing uncharacterized impurities [10,11]. For simulation, design and estimation of suitable operating parameters a theoretical study of the process described was carried out applying the equilibrium model and an equilibrium stage model.

2.1. Design equations based on equilibrium theory

The most important elements of the process described above are the two separation zones *II* and *III* and the solid phase regeneration zone *I*. The two additional zones for regeneration and equilibration also shown in Fig. 1 are decoupled from the main sections and can be easily designed independently. The correct functioning of zones *I–III* requires the identification and application of (a) an appropriate switching time, t^*, in the SMB process or (b) a corresponding solid phase flow rate applicable in the TMB process, $\dot{V}_S$, in combination with three internal, zone dependent liquid phase flow rates, $\dot{V}^z$. Hereby, the following balances connect the internal and external liquid phase flow rates:

$$\dot{V}^I = \dot{V}_D \tag{1}$$

$$\dot{V}^{II} = \dot{V}^I - \dot{V}_E \tag{2}$$

$$\dot{V}^{III} = \dot{V}^{II} + \dot{V}_F = \dot{V}_R \tag{3}$$

The essential free parameters of the process are three dimensionless flow rate ratios, m^z, for each zone *z*. These ratios are defined as [25–27]:

$$m^z = \frac{\dot{V}^z}{\dot{V}_S}, \quad z = I, II, III \tag{4}$$

Considering an isocratic separation of two components A and B characterized by linear adsorption isotherms:

$$q_i = H_i C_i, \quad i = A, B \quad \text{with} \quad H_A > H_B \tag{5}$$

the following inequalities define a region where a complete separation of A and B is possible [27]:

$$H_A < m^I \tag{6}$$

$$H_B < m^{II} < H_A \tag{7}$$

$$H_B < m^{III} < H_A \tag{8}$$

For the application of a two-step gradient in HIC-mode the salt concentration, C_{salt}, is set in the feed stream higher than in the desorbent stream, i.e. $C_{salt,F} > C_{salt,D}$ (Fig. 1b) [e.g. 31,32]. This leads to two different internal salt concentration levels in zones I/II and in zone III and consequently to two zone dependent Henry constants, H_i^z, for the two species A and B:

$$q_i = H_i^z C_i, \quad i = A, B;\ z = I/II, III \tag{9}$$

For the two compounds considered in this work (A: streptokinase, sk, B: degraded streptokinase and cellular contaminants, lumped below as impurities, im) in a limited range of salt concentrations the following linear dependence was observed (part I [23]):

$$H_i^z(C_{salt}^z) = a_{1,i} + a_{2,i} C_{salt}^z, \quad i = A(sk), B(im);\ z = I/II, III \tag{10}$$

For the Henry constants hold:

$$H_i^{I,II}(C_{salt}^{I,II}) = H_{i,D} < H_i^{III}(C_{salt}^{III}) = H_{i,R}, \quad i = A(sk), B(im) \tag{11}$$

The necessary conditions for complete separation are given for the two-step gradient three-zone TMB process by the following inequalities:

$$H_A(C_{salt}^{I,II} = C_{salt,D}) < m^I \tag{12}$$

$$H_B(C_{salt}^{I,II} = C_{salt,D}) < m^{II} < H_A(C_{salt}^{I,II} = C_{salt,D}) \tag{13}$$

$$H_B(C_{salt}^{III} = C_{salt,R}) < m^{III} < H_A(C_{salt}^{III} = C_{salt,R}) \tag{14}$$

The fixation of suitable internal salt concentrations in zone III, $C_{salt}^{III} = C_{salt,R}$, related to the corresponding entering salt concentrations, $C_{salt,F}$ and $C_{salt,D}$, is essential for the functioning of the process. Due to mass balance considerations, for the salt concentration in the raffinate stream [31–33] holds:

$$C_{salt,R} = \frac{\dot{V}_F C_{salt,F} + \dot{V}^{II} C_{salt,D}}{\dot{V}_R} \quad \text{with} \quad C_{salt,R} = [C_{salt,D}, C_{salt,F}] \tag{15}$$

Eq. (15) provides the following linear operation line in the (m^{II}, m^{III})-plane:

$$m^{III} = \frac{C_{salt,F} - C_{salt,D}}{C_{salt,F} - C_{salt,R}} m^{II} \tag{16}$$

The shape and size of the separation region is strongly affected by the Henry constants of the components (or fractions) that should be separated. For each specific separation problem and for given salt concentrations in the feed and the desorbent streams, there are two critical lines $L1$ and $L2$ and three critical points $P1$, $P2$ and $P3$ in the (m^{II}–m^{III}) plane. Expressions that specify the location of the separation region are given below. A corresponding illustration for the parameters valid for streptokinase (A) and the impurities (B) is given in Fig. 2.

The line $L1$ is fixed by the limit of fulfilling the lower boundary in Eq. (13) (i.e. $H_B(C_{salt,D}) = H_{B,D}$). This line fixes $P1$ by the intersection with the diagonal specifying the limit of no feed ($m^{II} = m^{III}$). To determine the location of line $L2$ a scanning of all possible $C_{salt,R}$ in the range between $C_{salt,D}$ and $C_{salt,F}$ is used. The specification of a concrete salt concentration in the raffinate stream, $C_{salt,R}^*$, leads to a critical Henry constant of component A (sk), $H_{sk,R}^{L2}$, given by Eq. (17):

$$H_{sk,R}(C_{salt,R}^*) = H_{sk,D} + (H_{sk,F} - H_{sk,D}) \frac{C_{salt,R}^* - C_{salt,D}}{C_{salt,F} - C_{salt,D}} \tag{17}$$

This Henry constant provides with the r.h.s. of Eq. (14) a corresponding critical value for $m^{III,L2}$ located on $L2$:

$$m^{III,L2}(C_{salt,R}^*) = H_{sk,R}(C_{salt,R}^*) \tag{18}$$

With this value and the equation for the operation line (Eq. (16)) it is finally possible to determine the corresponding $m^{II,L2}$ and, thus, a point on line $L2$:

$$m^{II,L2}(C_{salt,R}^*) = m^{III,L2}(C_{salt,R}^*) \frac{C_{salt,F} - C_{salt,R}^*}{C_{salt,F} - C_{salt,D}} \tag{19}$$

The whole line $L2$ can be determined using all critical values provided by Eqs. (17)–(19).

The point $P2$ is specified by the intersection of lines $L1$ and $L2$. Point $P3$ is found at the intersection of line $L2$ and the diagonal, $m^{II} = m^{III}$, corresponding also to $C_{salt,R} = C_{salt,D}$. For this point holds $m^{II} = H_{sk,D}$.

To fully define a concrete operating point the flow rate ratio m^I needs to be specified. Fulfilment of Eq. (12) can be achieved e.g. by transforming the inequality into an equality introducing a safety factor β^I:

$$m^I = \beta^I H_A(C_{salt,D}) \quad \text{with} \quad \beta^I > 1 \tag{20}$$

If an operating point is chosen within the described (m^{II}, m^{III}) separation region and if Eq. (20) is respected, equilibrium theory predicts that infinitely efficient columns will provide a purity $Pu_{i,Port}$ of 100% at both outlet ports with:

$$Pu_{i,Port} = \frac{C_{i,Port}}{\sum_j C_{j,Port}} 100\%, \quad i = sk, im;\ Port = E, R \tag{21}$$

2.2. TMB design based on an equilibrium stage model

Another simple model going beyond the possibilities of the equilibrium theory and being capable to describe steady state TMB processes is the equilibrium stage model suggested by Craig for the description of batch chromatography [34]. After adjusting the Craig model to the counter-current movement of the TMB process, the main mass balance equation for a component i and a stage or cell k located in zone z is [e.g. 29]:

$$\dot{V}^z(C_{i,k-1}^z - C_{i,k}^z) + \dot{V}_S(q_{i,k+1}^z(\bar{C}_{i,k+1}^z) - q_{i,k}^z(\bar{C}_{i,k}^z)) = \dot{V}_{ext} C_{i,ext} \tag{22}$$

with

$$\dot{V}_{ext} C_{i,ext} = \begin{cases} -\dot{V}_F C_{i,F} & \text{for } k = F \\ \dot{V}_E C_{i,E} & \text{for } k = E \\ 0 & \text{for all other } k \end{cases} \tag{23}$$

for

$$z = I, II, III, \quad i = A, B, \quad k = 1, N_{total}, \quad N_{total} = 4 + N^I + N^{II} + N^{III}$$

In the above $\dot{V}_{ext}$ and $C_{i,ext}$ are the external flow rate and concentrations in the liquid phase, N^z is the number of equilibrium stages in zone z and N_{total} is the number of equilibrium stages in the unit. For the solution of Eq. (22) again the knowledge of the distribution equilibrium is essential. For linear equilibrium functions there is a recursive solution available, which was suggested by Kremser [35] and adapted in [31] to allow calculating efficiently the concentrations at the zone outlets using aggregated forms of the mass balances [31,35,36]. The following two linear equations can be derived, which connect the inlet concentrations in each of

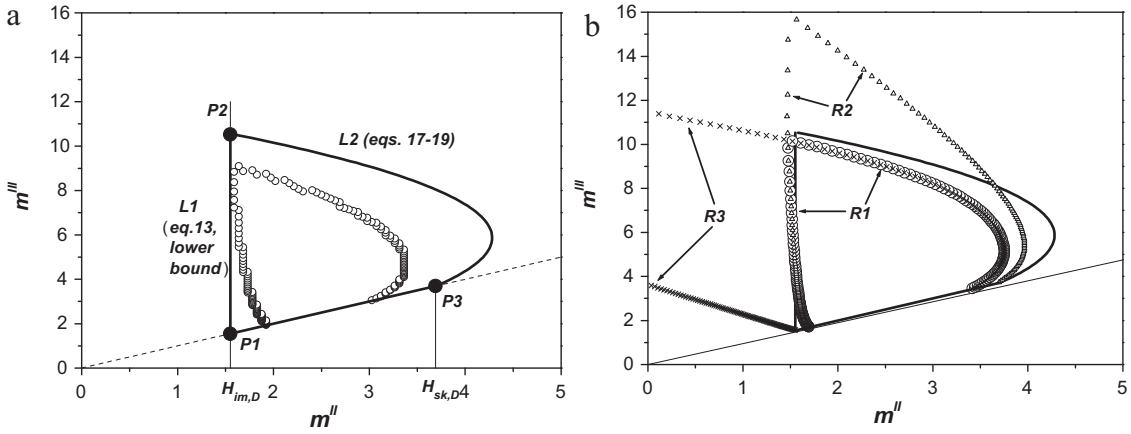

Fig. 2. Separation regions for $C_{salt,F}$ = 200 mM and $C_{salt,D}$ = 100 mM. Thick lines: equilibrium theory ($Pu_{sk,E} = Pu_{im,R} = 100\%$); (a) symbols: predictions of equilibrium stage model providing $Pu_{sk,E} = Pu_{im,R} \geq 99\%$ for $N^I = N^{II} = N^{III} = 20$ and $\beta^I = 2$; lines *L*1 and *L*2 and points *P*1, *P*2 and *P*3 as described in the text; (b) line: equilibrium theory (as in a); symbols: predictions of the equilibrium stage model, $N^I = N^{II} = N^{III} = 50$ and $\beta^I = 2$, *R*1: $Pu_{sk,E} = Pu_{im,R} \geq 99\%$ (circles); *R*2: $Pu_{sk,E} \geq 99\%$, $Pu_{im,R} \geq 70\%$ (triangles); *R*3: $Pu_{sk,E} \geq 70\%$, $Pu_{im,R} \geq 99\%$ (crosses).

the three zones, $C^z_{i,o}$ and C^z_{i,N^z+1} (z = *I*, *II*, *III*) with the corresponding concentrations in the first and last stages, $C^z_{i,1}$ and C^z_{i,N^z} [31,36]:

$$C^z_{i,N^z+1} = \gamma^z_i C^z_{i,1} - (\gamma^z_i - 1) C^z_{i,o} \tag{24}$$

$$C^z_{i,o} = \eta^z_i C^z_{i,N^z} - (\eta^z_i - 1) C^z_{i,N^z+1} \tag{25}$$

with

$$\gamma^z_i = \frac{(\chi^z_i)^{N^z+1} - 1}{\chi^z_i - 1} \tag{26}$$

$$\eta^z_i = \frac{(\chi^z_i)^{-(N^z+1)} - 1}{(\chi^z_i)^{-1} - 1} \tag{27}$$

and

$$\chi^z_i = \frac{\dot{V}^z}{\dot{V}_S H^{zz}_i} \quad \text{for } z = I, II, III;\ zz = \begin{cases} D & \text{for } z = I, II \\ R & \text{for } z = III \end{cases} \tag{28}$$

In addition the following four mass balances, valid for the characteristic inlet and outlet stages, have to be respected:

$$\text{Desorbent stage D}: \ C^I_{i,1^I} - (1 + \chi^I_i) C_{i,D} = 0 \tag{29}$$

$$\text{Extract stage E}: \ C^{II}_{i,1^{II}} + \chi^I_i C^I_{i,N^I} - \left(1 + \chi^{II}_i + \frac{\dot{V}_E}{\dot{V}_S H^{II}_i}\right) C_{i,E} = 0 \tag{30}$$

$$\text{Feed stage X}: \ C^{III}_{i,1^{III}} + \frac{H^{II}_i}{H^{III}_i} \chi^{II}_i C^{II}_{i,N^{II}} - (1 + \chi^{III}_i) C_{i,X} = -\frac{\dot{V}_F}{\dot{V}_S H^{III}_i} C_{i,X} \tag{31}$$

$$\text{Raffinate stage R}: \ C^{III}_{i,N^{III}} \chi^{III}_i - \left(1 + \frac{\dot{V}_R}{\dot{V}_S H^{III}_i}\right) C_{i,R} = 0 \tag{32}$$

For the three-zone open-loop gradient TMB process investigated, a system of 11 linear equations enables to calculate the concentrations for a component i in the first and last stages of each of the three zones. In the four characteristic stages D, E, F and R and in the characteristic stage where the solvent composition changes due to the gradient effect. If needed, the calculation of the whole internal concentration profiles can be easily performed using for each zone z the following equation [31]:

$$C^z_{i,n^z+1} = \gamma^z_i C^z_{i,1} - (\gamma^z_i - 1) C^z_{i,0} \quad \text{with } \gamma^z_i = \frac{(\chi^z_i)^{n^z+1} - 1}{\chi^z_i - 1} \text{ for } n^z = 1, 2, \ldots, N^z - 1 \tag{33}$$

As in the case of applying the equilibrium theory, attention has to be paid to the correct specification of the Henry constants as a function of the local salt concentrations (e.g. using Eq. (10)).

2.3. Equivalence between TMB and SMB

It is well known that there is significant equivalence between TMB and SMB processes [25–30]. Due to the much larger complexity of SMB models the above summarised simple TMB model provides a valuable basis for simulating SMB processes.

To transform the operating parameters identified as suitable for a hypothetical TMB process to corresponding parameters of a SMB process, the following analogy considerations can be used. The solid phase flow rate in the TMB process, $\dot{V}_S$, should be related to the SMB shift time, t^*, as follows:

$$t^* = \frac{V_{col}(1 - \varepsilon)}{\dot{V}_S} \tag{34}$$

or using the m^z-values

$$t^* = \frac{V_{col}(1 - \varepsilon) m^z}{\dot{V}^z_{TMB}}, \quad z = I, II, III \tag{35}$$

In Eqs. (34) and (35) V_{col} and ε are the volume and porosity of the chromatographic columns, respectively.

For the internal flow rates of the corresponding two simulated counter-current processes the following relations hold, providing the possibility to design the SMB process:

$$\dot{V}^z_{SMB} = \dot{V}^z_{TMB} + \frac{\dot{V}_S \varepsilon}{1 - \varepsilon} = \dot{V}_s \left(m^z + \frac{\varepsilon}{1 - \varepsilon}\right) = \frac{V_{col}(1 - \varepsilon)}{t^*} \left(m^z + \frac{\varepsilon}{1 - \varepsilon}\right), \quad z = I, II, III \tag{36}$$

For the technical realisation of the SMB process, in particular in a smaller scale, extra column volumes (or dead volumes) have to be taken into account. They contain additional storage capacities and affect the residence times of the components in the unit [37,38]. To consider additional dead volumes in zone z, V^z_d, the $\dot{V}^z_{SMB}$ have to be increased to assure the equality of the m^z-values:

$$\dot{V}^z_{SMB} = \dot{V}^z_{TMB} + \frac{\dot{V}_S \varepsilon}{(1 - \varepsilon)} + \frac{V^z_d}{t^*}, \quad z = I, II, III \tag{37}$$

To evaluate the process performance, the productivity, *PR*, can be used, which takes into account the concentration of the target component (here streptokinase, leaving the unit via the extract stream):

$$PR_E = \frac{C_{sk,E}\dot{V}_E}{N_{col}(1-\varepsilon)V_{col}} \quad (38)$$

3. Materials and equipment

The production of recombinant streptokinase, the application of discontinuous batch chromatography and the estimation of isotherms for Butyl Sepharose HP (HIC material provided by GE Healthcare) have been described in the first part of this communication. The SMB experiments were conducted using 2 mL columns per zone (two connected 1 mL columns). The average porosity of the columns was found using tracer experiments (purified streptokinase, 10 μL and 2 mg/mL, under non-binding conditions) to be $\varepsilon = 0.27 \pm 0.02$. An average number of equilibrium stages of the 1 mL column for streptokinase at a flow rate of 1.0 mL/min and the salt concentration range covered was $N = 10$, i.e. N^z is 20 for each zone [23]. The mobile phases in the feed and the desorbent were 20 mM phosphate buffers (pH 7.2) containing 200 mM and 100 mM $(NH_4)_2SO_4$, respectively. The cleaning in the regeneration zone (Fig. 1a) was done with Milli Q water at flow rate of 3 mL/min. As mobile phase in the equilibration zone was used a 20 mM phosphate buffer (pH 7.2) containing the same amount of $(NH_4)_2SO_4$ and having the same flow rate as the stream in zone *III*.

The SMB experiments were carried out with a CSEP 916 SMB unit (Knauer). The estimated dead volumes located in the fixed parts of the 16-port valve [11] and in the zones *I*–*III* were determined in preliminary tracer experiments as follows: $V_d^I = 1$ mL, $V_d^{II} = 1.7$ mL, $V_d^{III} = 1.2$ mL.

Raffinate and extract concentration profiles were measured using 2 Wellchrom K-2600 UV detectors (Knauer) at 280 nm. Additionally, UV_{280} and conductivity in zone *II* and after the regeneration zone were measured on-line using Amersham UPC-900 (GE Healthcare) detectors.

A more detailed analysis of the feed and the outlet fractions was done by SDS-PAGE and size exclusion chromatography. A quantitative estimation of the component concentrations and purity of the fractions was done applying SDS-PAGE (as described in the first part [23]). Qualitative analysis of the feed and the outlet fractions collected during the SMB experiments was done using size-exclusion chromatography with a Superdex 75™, 10/300 column (exclusion range 70 kDa, GE Healthcare). For this the column was pre-equilibrated with 50 mM Tris buffer (pH 8.2) containing 150 mM NaCl at a flow rate of 1 mL/min. Samples of 100 μL were injected. A description of the methods used to analyse the SMB runs is given in Section 4.2.

4. Results and discussion

4.1. Theoretical results: identification of the separation regions and parametric study

The continuous separation of streptokinase from cell lysate can be considered as a pseudo binary separation problem. In the first part of this communication, the corresponding adsorption equilibrium constants were estimated for different salt concentrations [23]. It was found that in a limited range between 100 mM and 200 mM $(NH_4)_2SO_4$ the effect of the salt concentration can be approximated by Eq. (10). The parameters estimated for streptokinase and the impurities are: $a_{1,sk} = -4.34$; $a_{2,sk} = 0.081\ \text{mM}^{-1}$, $a_{1,im} = 1.59$; $a_{2,im} = 0.0002\ \text{mM}^{-1}$.

For the realisation of the desired gradient conditions, the values for the salt concentrations in the feed and the desorbent stream were set in accordance with the range determined in the equilibrium investigations as $C_{salt,F} = 200$ mM and $C_{salt,D} = 100$ mM. Eq. (10) provides the following characteristic Henry constants: $H_{sk,D} = H_{sk,II} = 3.76$, $H_{im,D} = H_{im,II} = 1.61$, $H_{sk,F} = 11.86$, $H_{im,F} = 1.63$.

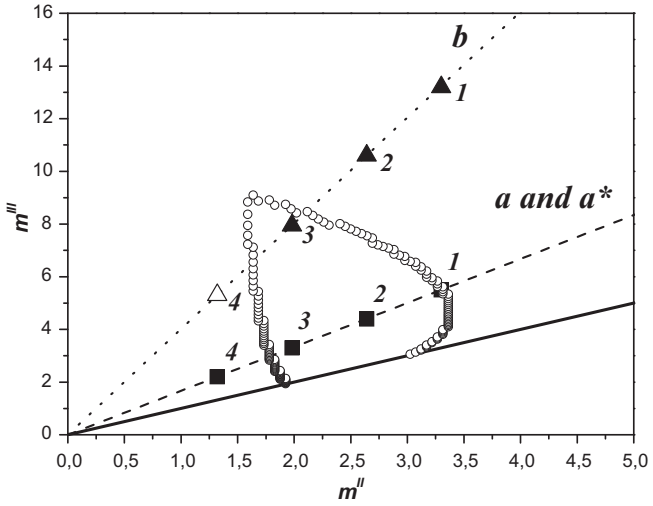

Fig. 3. Separation region in the (m^{II}, m^{III}) plane for the separation of streptokinase using the equilibrium stage model with $N^I = N^{II} = N^{III} = 20$ (circles) and the experimentally realised operating points for operation lines *a* (dashed, line *a*, $\beta^I = 2$ and *a**, $\beta^I = 1.1$) and *b* (dotted, $\beta^I = 2$). Characteristic values for the marked operating points are listed in Table 1.

To estimate the operating region a relatively large safety value for zone one was chosen ($\beta^I = 2$). Using this value and the strategy described in the theoretical part, a region of complete separation in the (m^{II}, m^{III}) plane can be estimated. A graphical representation is shown in Fig. 2a. For the estimation of this region at first the equilibrium model (i.e. an infinitely efficient system) was used. The region allowing 100% purity is defined by the two lines *L*1 and *L*2 and the three points *P*1, *P*2 and *P*3. In parallel, a region calculated with the equilibrium stage model is also presented in Fig. 2a. In the results given, the number of theoretical plates available in the real system ($N^I = N^{II} = N^{III} = 20$) and a 99% purity at both outlet streams were used as constraints. Comparing both regions, the lower efficiency leads to a shrinking of the separation region calculated with the equilibrium stage model.

Similar screening in the (m^{II}, m^{III}) plane was done by increasing the number of equilibrium stages for each zone ($N^I = N^{II} = N^{III} = 50$) and verifying the purity constrains for the outlets. The estimated regions predicted by the equilibrium stage model are depicted in Fig. 2b. For comparison the region for the ideal situation is also presented in the figure. Comparing the regions predicted with the equilibrium stage model for 20 (Fig. 2a) and 50 plates (Fig. 2b, *R*1) revealed an expected increase of the size of the region for higher plates number. For region *R*2 the purity constraints in the extract and raffinate streams were set to $Pu_{sk,E} = 99\%$ and $Pu_{im,R} = 70\%$. Another screening (region *R*3) was done for assumed purities of $Pu_{sk,E} = 70\%$ and $Pu_{im,R} = 99\%$. Both regions with reduced purity requirements are larger than region *R*1 providing an increasing number of available operating parameters. The shape of the *R*1 and *R*2 regions is similar. In comparison to region *R*1 the location of the regions *R*2 and *R*3 shift in the (m^{II}, m^{III}) plane towards the theoretical zones of pure raffinate (up, higher m^{III} values) or pure extract (left, lower m^{II} values).

To investigate the separation performance, a parametric study for different operating conditions was carried out. Based on the theoretical screening, two times four operating points located on two operation lines for $C^a_{salt} = 140$ mM and $C^b_{salt} = 175$ mM were selected. The region and the corresponding lines and points are

Table 1
Summary of the parameters used for the simulation study and purity of the extract port using the TMB model (Figs. 3 and 4). $\dot{V}_F = 1$ mL/min.

Point nr.	$C_{salt,R}$ [mM]	m^I	m^{II}	m^{III}	$\dot{V}_S$ [mL/min]	$\dot{V}_D$ [mL/min]	$\dot{V}_E$ [mL/min]	$\dot{V}_R$ [mL/min]	$Pu^{th}_{sk,E}$ [%]
1^a	140	7.41[1]	3.30	5.5	0.45	3.42	1.92	2.50	100
2^a	140	7.41[1]	2.64	4.4	0.57	4.27	2.77	2.50	100
3^a	140	7.41[1]	1.98	3.3	0.76	5.70	4.20	2.50	99.9
4^a	140	7.41[1]	1.32	2.2	0.57	8.54	7.04	2.50	78.9
1^b	175	7.41[1]	3.30	13.2	0.10	0.76	0.43	1.33	100
2^b	175	7.41[1]	2.64	10.6	0.13	0.94	0.61	1.33	100
3^b	175	7.41[1]	1.98	7.95	0.17	1.26	0.93	1.33	100
4^b	175	7.41[1]	1.32	5.3	0.25	1.86	1.53	1.33	94.4
1^{a*}	140	4.08[2]	3.30	5.5	0.45	1.88	0.38	2.50	100
2^{a*}	140	4.08[2]	2.64	4.4	0.57	2.35	0.85	2.50	100
3^{a*}	140	4.08[2]	1.98	3.3	0.76	3.13	1.63	2.50	99.9
4^{a*}	140	4.08[2]	1.32	2.2	0.57	4.67	3.12	2.50	78.8

[1] $\beta^I = 2$.
[2] $\beta^I = 1.1$.

depicted in Fig. 3. The corresponding values for the operating points are summarised in Table 1. The study was done using the equilibrium stage model (Eq. (22)). For the calculations performed, the feed mixture considered had the following concentrations $C_{im,F} = C_{sk,F} = 5$ mg/mL. The feed flow rate was set to $\dot{V}_F = 1$ mL/min. All calculations were done for columns providing cell number of 20 per zone. The calculated internal concentration profiles are shown in Fig. 4. The concentration of the components in the feed mixture and the position of the inlet and outlet ports are marked. The theoretical concentrations of streptokinase at the extract port and of the impurities at the raffinate port are also marked. For the selected points the effect of the salt concentration on the product concentration was studied. The safety factor for zone I was $\beta^I = 2$. The accomplished study shows that for the points at line a ($C^a_{salt} = 140$ mM) there is a dilution at the extract port in comparison with the feed concentration. A comparison between the

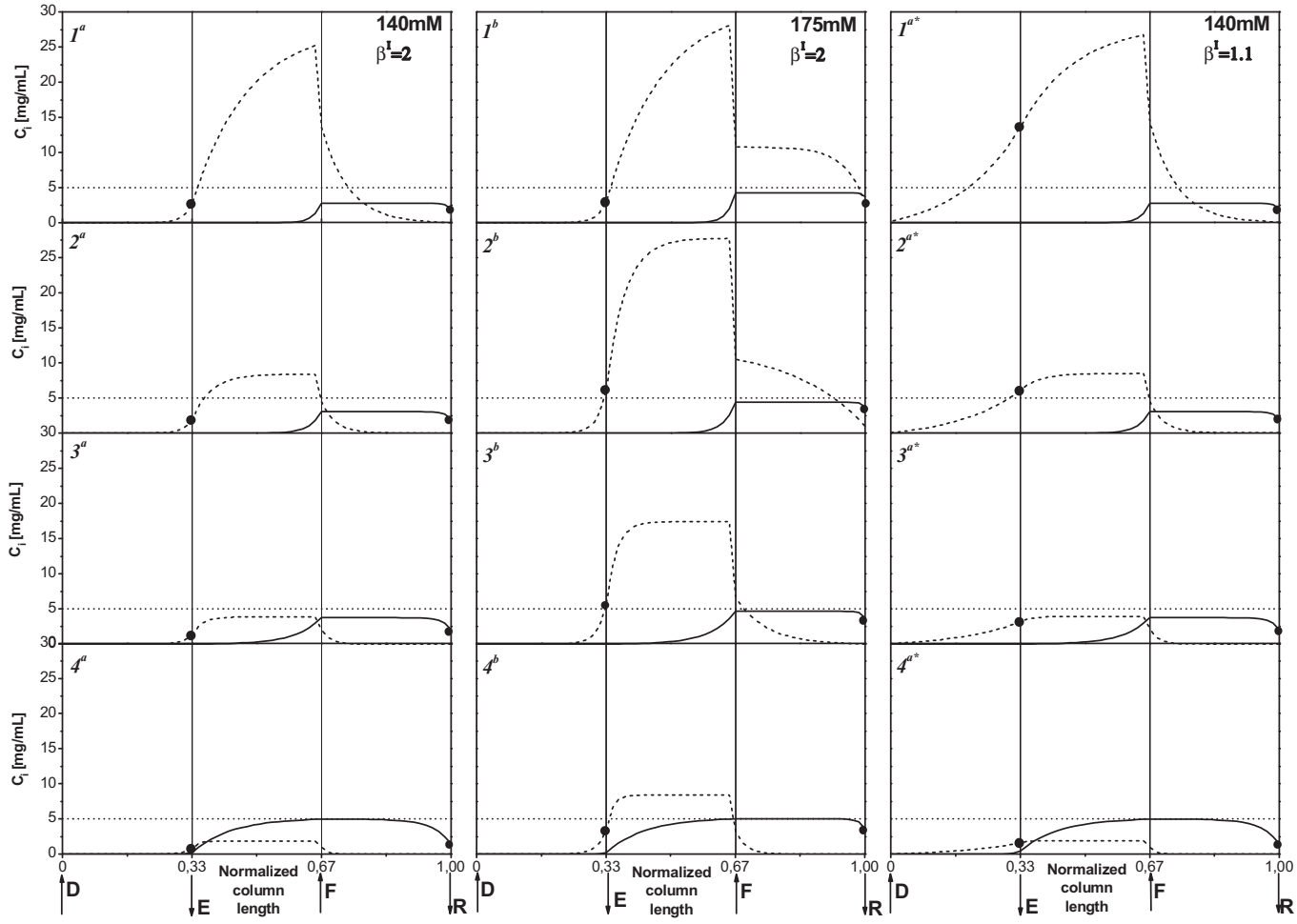

Fig. 4. Simulated internal concentration profiles for the separation of streptokinase at different operating conditions. Left: for operation line a and $\beta^I = 2$. Middle: for operation line b and $\beta^I = 2$. Right: for operation line a^* and $\beta^I = 1.1$. The dashed and solid lines indicate the profiles of the streptokinase and the impurities, respectively, for $N^I = N^{II} = N^{III} = 20$. The thin horizontal dotted lines mark the feed concentrations considered, $C_{sk,F} = C_{im,F} = 5$ mg/mL. The arrows indicate the positions of the desorbent (D), extract (E), feed (F) and raffinate (R) ports. The dots mark the streptokinase and impurity concentrations at the extract and raffinate ports, respectively.

Table 2
Summary of the experimentally applied parameters (Figs. 5–8). $\dot{V}_F = 1.0$ mL/min, except $\dot{V}_F = 0.5$ mL/min for point 4^{a*}. The external flowrates are based on Eq. (37) considering dead volumes. The m^z-values are given in Table 1.

Point nr.	t^* [min]	$\dot{V}_{D,SMB}$ [mL/min]	$\dot{V}_{E,SMB}$ [mL/min]	$\dot{V}_{R,SMB}$ [mL/min]	$C^{th}_{sk,E}$ [mg/mL]	$C^{exp}_{sk,E}$ [mg/mL]	$C^{th}_{sk,R}$ [mg/mL]	$C^{exp}_{im,sk,R}$ [mg/mL][1]	$Pu^{th}_{sk,E}$ [%][2]	$Pu^{exp}_{sk,E}$ [%]
1^b	13.9	0.87	0.37	1.46	2.97	0.33	2.84	6.60	100	56.0
2^b	11.1	1.09	0.55	1.49	6.15	0.31	1.01	6.44	100	57.0
3^b	8.4	1.45	0.84	1.55	5.51	0.44	0.02	7.31	100	76.9
1^{a*}	3.1	2.39	0.15	3.08	13.6	0.34	0.13	5.94	100	69.8
2^{a*}	2.5	3.00	0.57	3.23	6.07	0.50	0.05	6.23	100	78.2
3^{a*}	1.8	4.00	1.25	3.47	3.14	0.98	0.02	5.80	99.9	83.6
4^{a*}	2.5	3.00	1.32	1.98	1.60	1.42	0.01	7.75	78.8	72.8

[1] Total protein concentration estimated by the BCA method.
[2] Equilibrium stage model, $N^I = N^{II} = N^{III} = 20$.

concentrations of the target component at this port shows a clear decreasing trend from point 1^a to 4^a, i.e. moving down at the operation line. In contrast, for the points at line b ($C^b_{salt} = 175$ mM) the concentrations at the extract outlet are higher than at line a, but only for point 2^b and 3^b they are higher than in the feed. The purity of streptokinase is less than 100% only for points 4^a and 4^b (Table 2). Regarding the raffinate port, at operation line a the purity is 100%. For operation line b there is loss of streptokinase at this port. Moving down the operation line b from point 1^b to 4^b the amount of lost product decreases. At both operation lines the concentration of the impurities decreases in comparison with their concentration in the feed solution, but remains constant in the raffinate stream.

To evaluate the effect of the safety factor in zone I, additional calculations were performed for line a by reducing its value to $\beta^I = 1.1$. This is connected with a decrease of the desorbent flow rate. There is the expected increase of the streptokinase concentration at the extract port in comparison with the estimated values for the same line and $\beta^I = 2$ (Fig. 4, left). For both cases the purity at this port is 100%, except for points 4^{a*} and 4^a. For point 1^{a*} the highest target concentration is found. The theoretical enrichment factor ishere

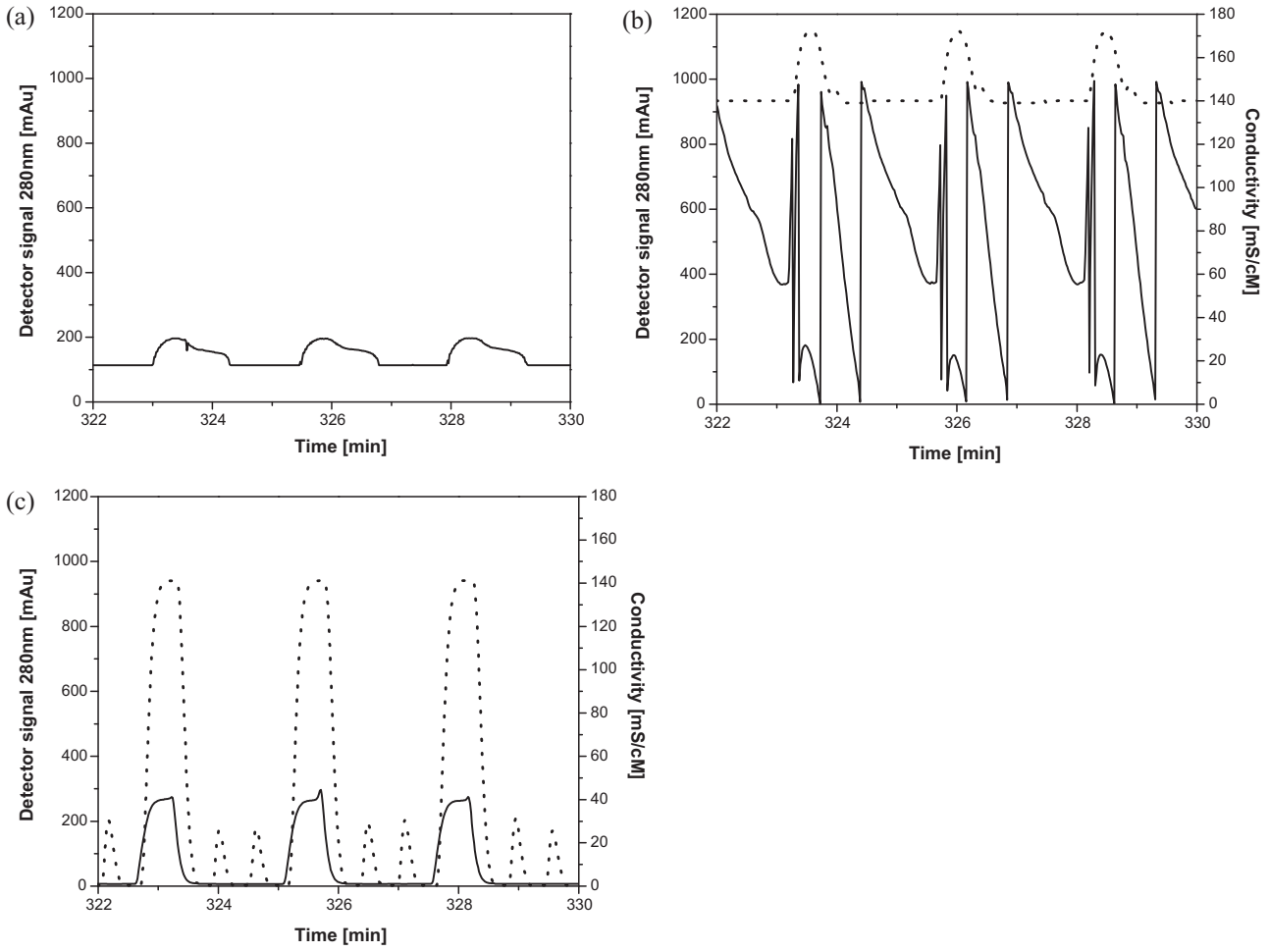

Fig. 5. Online UV_{280} and conductivity profiles measured for the run corresponding to point 2^{a*} (operation line a in Fig. 3) after reaching the cyclic steady state ($t^* = 2.5$ min). (a) Profile at extract outlet; (b) UV_{280} (solid) and conductivity (dotted) profiles at end of zone II; (c) UV_{280} and conductivity profiles at the end of the cleaning zone.

almost 3 (Fig. 4, right, top). Regarding the raffinate port, there is no severe influence of the safety factor on purity (i.e. loss of target streptokinase) and impurity concentration.

4.2. Experimental results

To validate the results obtained from the theoretical investigations, seven SMB experiments were carried out. In agreement with the operating points evaluated theoretically, the operating parameters were located on the two operation lines a^* (C^a_{salt} = 140 mM) and b (C^b_{salt} = 175 mM) given in Fig. 3. The safety factors chosen for zone I were $\beta^I = 2$ for line b and $\beta^I = 1.1$ for line a^*. The total protein concentrations, $C_{sk,F} + C_{im,F}$, in the feed were 17.2 mg/mL for line a^* and 10.6 mg/mL for line b. The values for the three dimensionless flow rates, m^z, were the same as in the corresponding theoretical investigations (Table 1, Fig. 3). In all runs the feed flow rates were 1 mL/min. To overcome flow rate restrictions of the columns used (up to 4 mL/min), a reduced feed flow rate of $\dot{V}_F = 0.5$ mL/min was set for operating point 4^{a*}. To design the experiments the extra column dead volumes, $\dot{V}^z_d$, were taken into account using Eq. (37). The external flow rates calculated for all SMB experiments carried out are summarised in Table 2.

In carrying out the experiments, after indication of the cyclic steady state based on the UV signals at 280 nm and corresponding conductivity signals, samples were taken at the raffinate and extract ports over a multiple of shift times. A typical example for the run corresponding to point 2^{a*} is depicted in Fig. 5. All three plots shown demonstrate that the cyclic steady state was reached. Samples collected at the extract and raffinate ports were analysed by the methods described in Part I of this communication [23]. A comparison of the elution profiles (SEC-analysis) of the extract samples of all seven runs is shown in Fig. 6. The target component streptokinase can be recognized at a retention volume of 10 mL. Because of the relatively large number of impurities, the corresponding raffinate fractions were not analysed by SEC-chromatography. The purities of both outlets (extract and raffinate) were determined by SDS-PAGE. Subsequently, an estimation of the corresponding streptokinase concentration in the target (extract) stream was done also using SDS-PAGE results. The high number of components present in the feed (cell lysate) and in all raffinate fractions hindered the usage of this method for the estimation of the corresponding streptokinase concentrations. For feed and raffinate only the total protein concentrations were determined by the BCA method (Bi-Cinchoninic Acid, Part I of this communication [23]). The SDS-PAGE results for all experimental points are presented in Fig. 7. The

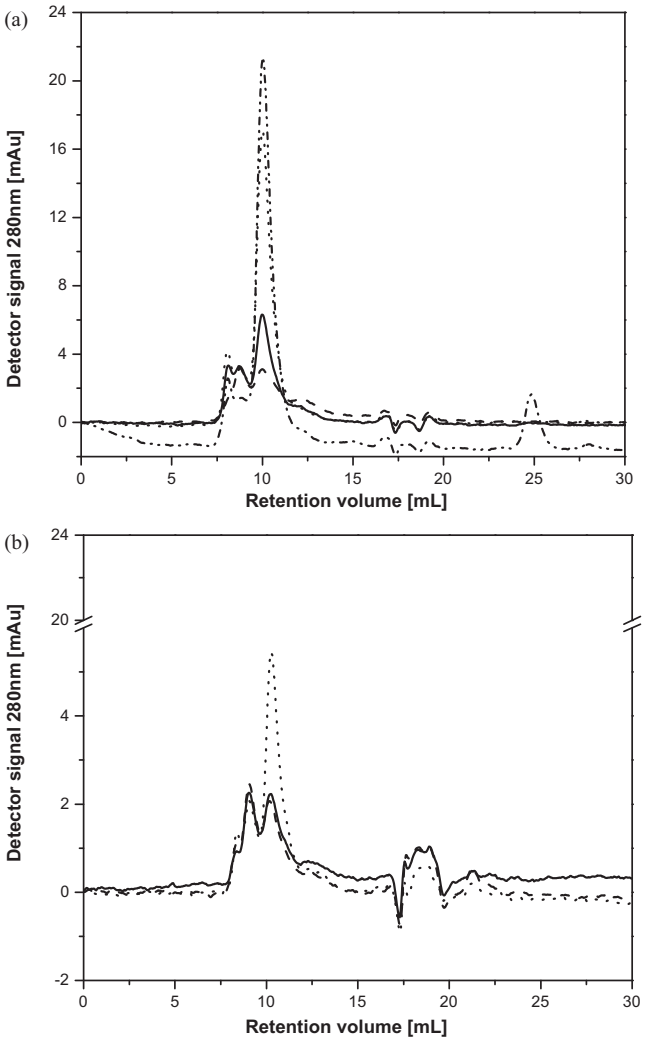

Fig. 6. SEC analysis of the seven SMB runs, fractions collected at the extract port. (a) Line a^* ($\beta^I = 1.1$) and operating points 1^{a*} (dashed), 2^{a*} (solid), 3^{a*} (dotted), 4^{a*} (dash-dotted); (b) line b ($\beta^I = 2$) and operating points 1^b (dashed), 2^b (solid), 3^b (dotted).

experimentally estimated values for the purities, $Pu^{exp}_{sk,E}$, and the streptokinase concentrations, $C^{exp}_{sk,E}$, are summarised in Table 2.

Comparing all experiments conducted, the highest streptokinase purity levels achieved were for runs 2^{a*} and 3^{a*}, 78.2% and 83.6%, respectively (Table 2). The corresponding operating

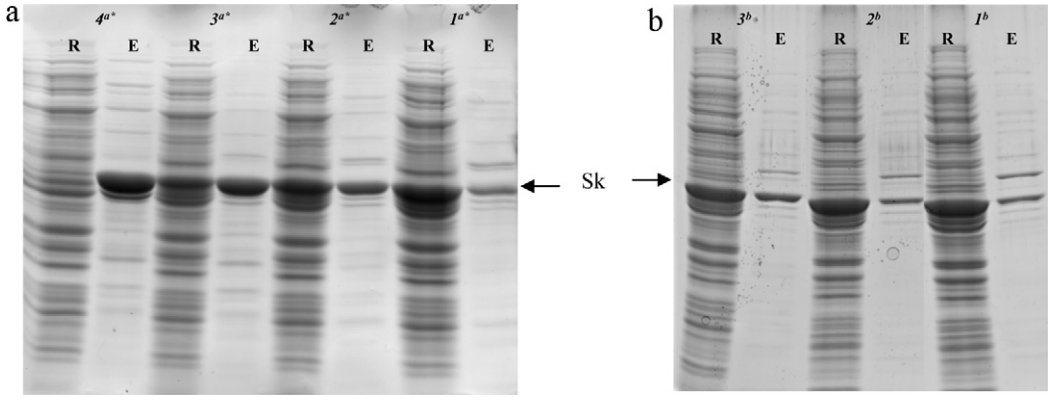

Fig. 7. SDS-PAGE analysis of the extract (E) and raffinate (R) outlets for all seven runs (Table 2). (a) operation line a^* ($\beta^I = 1.1$); (b) operation line b ($\beta^I = 2$).

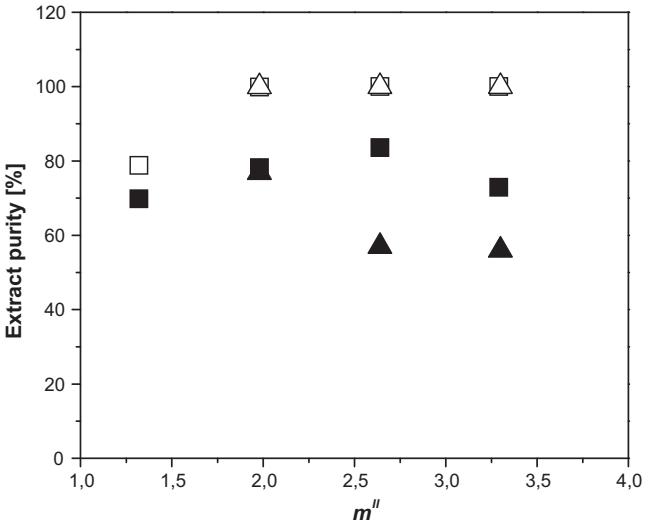

Fig. 8. Experimental (closed symbols) and theoretical (open symbols) purities of extract as function of m^{II} for the seven SMB runs. Lines a^* (squares, $\beta^I = 1.1$, 1^{a*}, 2^{a*}, 3^{a*}, 4^{a*}) and b (triangles, $\beta^I = 2$, 1^b, 2^b, 3^b). The experimental data and values used are shown in Figs. 5–7 and Table 2.

points are located on line a^* and inside the estimated separation region (Fig. 3). For these two points an undesired loss of streptokinase was found at the raffinate port (see SDS-PAGE results in Fig. 7a).

Three of the operating points, 1^b and 2^b ($C^b_{salt} = 175$ mM) and 4^{a*} ($C^{a^*}_{salt} = 140$ mM), were located outside of the estimated separation region. For points 1^b and 2^b the lowest purities and product concentrations were obtained, 56% and 57% with 0.33 and 0.31 mg/mL of streptokinase, respectively. In contrast, the highest experimental value of product concentration, 1.42 mg/mL, related to relative high streptokinase purity of 72.8% was achieved for the operating point 4^{a*} (Fig. 7, Table 2). This result corresponds to a productivity, PR (Eq. (38)), of 0.48 g/($L_{stationary\ phase}$·min). For all three points, 1^b, 2^b and 4^{a*}, in the fractions collected at the extract port uncharacterized high molecular weight impurities were found. There was again a significant amount of product loss in the raffinate port (Fig. 7).

The theoretically expected and the experimentally determined values for the purities and concentrations of streptokinase at the extract port differ significantly, especially for points 1^b, 2^b and 1^{a*} (Table 2 and Fig. 8). For the above discussed relatively successful runs 2^{a*}, 3^{a*} and 3^b the agreement is slightly better. The best agreement is found for run 4^{a*} located outside the separation region (Fig. 3).

The reasons for the deviations between experimental results and predictions are complex. The salt gradients applied might be in reality not as perfect as assumed in the model. In the internal concentration profiles calculated with the described TMB model the dead volumes of the experimental unit were not taken into account. These volumes were included only during specifying the operating parameters. The TMB model itself must be seen as a rather coarse approximation for a SMB process using just 3 columns. Further, the validity of linear isotherms and the correctness of the isotherm parameters determined was assumed. The calculated theoretical profiles presented in Fig. 4 show rather high streptokinase internal concentrations, which might be in a nonlinear region of the isotherms. Therefore the extrapolation of the isotherm parameters is questionable. Another strong and doubtful simplification made is the application of an averaged plate number for all flowrates and salt concentrations. All aspects mentioned before can be reasons, why there was in all experiments a not predicted loss of streptokinase at the raffinate port. These losses increase moving down the operation lines, e.g. from points 1^{a*} or 1^b to points 4^{a*} or 3^b (see Fig. 7). This experimental result suggests that collecting and further recycling of the raffinate port fraction is useful to improve the separation studied.

5. Conclusions

In this work the application of a simple concept for the continuous purification of recombinant streptokinase from cell lysate by three-zone open-loop two-step gradient SMB process was investigated.

In the first part of this communication the adsorption isotherms of the key components at different salt concentrations were determined. For the components considered the estimated isotherms were found to be rather linear. Over a limited salt concentration range also a linear dependence of the adsorption isotherm parameters holds. This thermodynamic information, the equilibrium theory and an equilibrium stage model (Craig model) were used to screen the (m^{II}, m^{III}) plane for suitable operating regions of a three-zone open-loop SMB process. Based on a simulation study, the behaviour of the system was analysed. For specified operating parameters internal concentration profiles were calculated to show the effect of the salt gradient. The obtained theoretical results were the basis for the realization of seven SMB experiments. In some runs the target component streptokinase could be separated from the impurities present in the cell lysate with relatively high purity. The theoretically predicted enrichment of streptokinase due to the step gradient was not reached in the experiments. Comparing the theoretical and experimental values regarding the purity, similar trends were found. Possible reasons for the observed quantitative discrepancies were identified. Depending on the purity and yield constraints the described continuous purification process can be applied for initial capture or intermediate purification of recombinant streptokinase.

Acknowledgements

We acknowledge the support of the Bioprocess Engineering Group at the MPI and the Leibniz Institute for Neurobiology (both in Magdeburg). S.P. acknowledges the financial support of Deutscher Akademischer Austauschdienst (DAAD) and the travel grant to the "HPLC 2009" from GDCh. The support of Deutsche Forschungsgemeinschaft via "SFB 578" is also gratefully acknowledged.

References

[1] N. Ferrer-Miralles, J. Domingo-Espin, J.L. Corchero, E. Vazquez, Microb. Cell Fact. 8 (2009) 17.
[2] J.E. Dyr, J. Suttnar, J. Chromatogr. B 699 (1997) 383.
[3] X.D. Geng, L.L. Wang, J. Chromatogr. B 866 (2008) 133.
[4] A.K.S. Babu, M.A. Vijayalakshmi, Biotechnol. J. 4 (2009) 1132.
[5] A. Rajendran, G. Paredes, M. Mazzotti, J. Chromatogr. A 1216 (2009) 709.
[6] M. Juza, M. Mazzotti, M. Morbidelli, Trends Biotechnol. 18 (2000) 108.
[7] E.R. Francotte, P.P. Richert, J. Chromatogr. A 769 (1997) 101.
[8] A. Seidel-Morgenstern, L.C. Keßler, M. Kaspereit, Chem. Eng. Technol. 31 (2008) 826.
[9] S. Mun, Y. Xie, N.-H.L. Wang, Ind. Eng. Chem. Res. 44 (2005) 3268.
[10] L. Gueorguieva, L.F. Vallejo, U. Rinas, A. Seidel-Morgenstern, J. Chromatogr. A 1135 (2006) 142.
[11] L.C. Keßler, L. Gueorguieva, U. Rinas, A. Seidel-Morgenstern, J. Chromatogr. A 1176 (2007) 69.
[12] J. Houwing, H.A.H. Billiet, L.A.M. van der Wielen, J. Chromatogr. A 944 (2002) 189.
[13] G. Paredes, S. Makart, J. Stadler, M. Mazzotti, Chem. Eng. Technol. 28 (2005) 1335.
[14] N. Gottschlich, S. Weidgen, V. Kasche, J. Chromatogr. A 719 (1996) 267.
[15] S. Abel, M.U. Bäbler, C. Arpagaus, M. Mazzotti, J. Stadler, J. Chromatogr. A 1043 (2004) 201.
[16] N. Gottschlich, V. Kasche, J. Chromatogr. A 765 (1997) 201.

[17] D.A. Horneman, M. Ottens, J.T.F. Keurentjes, L.A.M. van der Wielen, J. Chromatogr. A 1113 (2006) 130.
[18] D. Sahoo, J. Andersson, B. Mattiasson, J. Chromatogr. B 877 (2009) 1651.
[19] D.A. Horneman, M. Ottens, J.T.F. Keurentjes, L.A.M. van der Wielen, J. Chromatogr. A 1157 (2007) 237.
[20] A. Seidel-Morgenstern, Chem. Eng. Technol. 28 (11) (2005) 1265.
[21] L.R. Snyder, M.A. Stadalius, in: C. Horvath (Ed.), High Performance Liquid Chromatography – Advances and Perspectives, vol. 4, Academic Press, New York, 1986, p. 208.
[22] P. Jandera, J. Churacek, Gradient Elution in Column Liquid Chromatography, Elsevier, Amsterdam, 1985.
[23] S. Palani, L. Gueorguieva, U. Rinas, A. Seidel-Morgenstern, G. Jayaraman, J. Chromatogr A 1218 (2011) 6396.
[24] H.K. Rhee, R. Aris, N.R. Amundson, Philos. Trans. Roy. Soc. London A 267 (1970).
[25] M. Mazzotti, G. Storti, M. Morbidelli, AIChE J. 40 (1994) 1825.
[26] M. Mazzotti, G. Storti, M. Morbidelli, AIChE J. 42 (1996) 2784.
[27] M. Mazzotti, G. Storti, M. Morbidelli, J. Chromatogr. A 769 (1997) 3.
[28] D.M. Ruthven, C.B. Ching, Chem. Eng. Sci. 44 (1989) 1011.
[29] G. Guiochon, S. Golshan-Shirazi, A.M. Katti, Fundamentals of Preparative and Nonlinear Chromatography, Academic Press, New York, 2006.
[30] C.B. Broughton, C.G. Gerhold, US Patent, 2,985,589, 1961.
[31] D. Beltscheva, P. Hugo, A. Seidel-Morgenstern, J. Chromatogr. A 989 (2003) 31.
[32] D. Antos, A. Seidel-Morgenstern, J. Chromatogr. A 944 (2002) 77.
[33] S. Abel, M. Mazzotti, M. Morbidelli, J. Chromatogr. A 944 (2002) 23.
[34] L.C. Craig, J. Biol. Chem. 155 (1944) 519.
[35] A. Kremser, Nat. Petroleum News 22 (1930) 42.
[36] L.C. Keßler, A. Seidel-Morgenstern, J. Chromatogr. A 1126 (2006) 323.
[37] C. Migliorini, M. Mazzotti, M. Morbidelli, AIChE J. 45 (1999) 1411.
[38] S. Katsuo, C. Langel, P. Schanen, M. Mazzotti, J. Chromatogr. A 1216 (2009) 1084.